Achieving a Peak Capacity of 1800 Using an 8 m Long Pillar Array Column

Baca, Martyna; Desmet, Gert; Ottevaere, Prof. Dr. Ir. Heidi; De Malsche, Wim

Published in:
Analytical Chemistry

DOI:
10.1021/acs.analchem.9b02236

Publication date:
2019

License:
Other

Document Version:
Proof

Achieving a peak capacity of 1800 using an 8 m long pillar array column

Martyna Baca[1], Gert Desmet[1], Heidi Ottevaere[2] and Wim De Malsche[1] *

[1]Vrije Universiteit Brussel, Department of Chemical Engineering, Brussels, Belgium

[2]Vrije Universiteit Brussel, Department of Applied Physics and Photonics, Brussels, Belgium

(*) corresponding author

Pleinlaan 2, B-1050, Brussels, Belgium

Abstract

In the present study, the peak capacity potential of ultra-long porous cylindrical pillar array columns is investigated. Coupling 4 columns of 2 m long allows to work near the minimal separation impedance of small molecules under retained conditions at a maximal pressure load of 250 bar. Minimal plate heights of H=5.0 µm, H=6.3 µm and H=7.7 µm were obtained for uracil (unretained), butyrophenone (k=0.85), valerophenone (k=1.94) respectively, corresponding to a number of theoretical plates N=1.6×10^6, N=1.2×10^6 and N=1.0×10^6. The optimal linear velocities were 0.60 mm/s for the retained compounds and 0.74 mm/s for the unretained compound. Based on a mixture of 9 compounds, the peak capacity n_c was determined as a function of gradient time (t_G). Peak capacities (t_G-based) of 1103 and 1815 were obtained when applying 650-min and 2050-min gradients (t_G/t_0 = 4.5 and 14, respectively, with t_G the gradient time and t_0 the void time). These values are much higher than earlier reported peak capacity values for small molecules.

1. Introduction

Since the emergence of chromatographic columns, most efforts in performance improvement have been predominantly devoted to the reduction of the particle size, columns size and domain size for the respective packed bed, open tubular and monolithic column formats [1,2,3]. This trend has been driven by the fact that, under ideal conditions, the plate height scales with a representative characteristic dimension [4]. This evolution has led to the emergence of faster performing columns for most relevant sample complexities (<few 100 peaks) [5]. In parallel, also improvements in packing quality have been realized, which led to the emergence of fully ordered pillar array columns wherein the particles are replaced by lithographically structured silicon pillars [6,7]. Micro-fabricated packings have the advantage that also the permeability

can be easily reduced, due to the design freedom in pillar positioning and shape [8]. This allows for a minimization of the separation impedance [9,10]. Our group and several other groups have developed a wide range of pillar array columns configurations and dedicated fabrication methods for several column substrates [11-15]. Also monolithic columns are well appreciated for their high permeability but cannot compete with packed (and pillar array) columns in terms of plate height [16]. The latter aspect has however, somehow surprisingly, not impeded that large peak capacities have been demonstrated with (polymeric) monolithic columns using large molecules [17], due to the abrupt desorption behavior (related to the large solvent strength value S) of e.g. proteins and peptides in these columns. Typical peak capacities for peptide separation (using conventional LC) range between 100 and 400 for analysis times between 30 min up to 1 h [18,19], higher peak capacities (>500) have been achieved when long gradient times are applied. A peak capacity of 1360 was achieved for the separation of tryptic digest of β-lactoglobulin and six proteins, using 900 mm long coupled column systems packed with 2.6 µm core–shell particles, applying a 480 min gradient (with the solvent strength S= 25, the change in solvent composition from the beginning to the end of the gradient run time Δc= 0.5, t_G/t_0= 52) [17]. Horie *et al.* reported the maximal peak capacity of 1600 for peptide separations obtained on 3.5 m×100 µm silica monolith column, applying a gradient of 2400 min [20]. Guillarme *et al.* reported on a packed column (150 mm × 2.1 mm) wherein a peak capacity of 1120 was realized in only 1.5h, applying ultra-high-pressure and high-temperature (90 ºC) conditions [21]. Rogeberg *et al.* achieved a peak capacity of 185 within 90 min for the separation of intact proteins with a 10 µm i.d. 3 m porous layer open tubular polystyrene divinylbenzene column [22]. Hara *et al.* demonstrated an excellent efficiency using octadecylsilylated silica-based porous layered open tubular (PLOT) columns with an inner diameter (i.d.) of 5 µm and with a layer thickness (d_f) of 250 nm and a column length of 0.4 m. A good performance was reported, achieving for the most retained compound (k = 0.9–1.5)

column efficiency N = 101,000 [23]. Hara *et al.* also reported much higher efficiency separations using 5 µm i.d. porous silica layer open-tubular 0.6 m long capillaries coated with a mesoporous silica layer produced by another sol-gel recipe thickness of 550 nm. These columns allowed for efficiencies of up to N = 600 000 plates (90 min) for a retained and around N = 1 000 000 plates for an unretained component (obtained in 50 min) [24]. The gain in peak capacity per time unit is less than what can be conceptually obtained using comprehensive 2D-LC. Nevertheless, even 2D separations are ultimately limited by the efficiency of the chromatographic column in the individual dimensions. Furthermore, the separation power of 1D-LC is essential to resolve chiral or isotope samples and an additional orthogonal retention mechanism does generally not further contribute to resolution in these cases. For mixtures that do benefit from a second dimension, impressive values have been obtained with 2D-LC. Sarrut et al. reported e.g. on RPLC × RPLC (1D-Ascentis Express C18, 50 × 2.1 mm, 2.7 µm; 2D-Kinetex C18, 30 × 2.1 mm, 1.3 µm) separations of a protein digest yielding an effective peak capacity ($n_{2d,eff}$) of 5100 when applying a gradient of 200 min (with S=0.2, $\Delta c,1D$ = 0.3, $\Delta c,2D$ = 0.43) [25].

In recent work, we demonstrated large (unretained) plate counts (N= 1 × 10^6) in porous pillar array columns containing 5 µm cylindrical pillars with a spacing of 2.5 µm. The column length was 2 m, which was about 4 time slower than the kinetic optimal length, at which the maximal number of plates can be produced per unit of time [26]. In the present work, we couple 4 such columns to study the maximal attainable peak capacity of small molecules in such a 5 µm pillar diameter system.

2. Materials and methods.

2.1 Chemicals and materials.

Acetanilide (≥99.9%), acetophenone (≥99.0%), propriophenone (≥99.0%), butyrophenone (≥99.0%), valerophenone (≥99.0%), hexanophenone (≥99.0%), heptanophenone (98%), octanophenone (≥99.0%), formic acid (≥99.0%), uracil (≥99.0%) were purchased from Sigma-Aldrich (Diegem, Belgium). Acetonitrile (HPLC Supra-gradient) was purchased from Biosolve (Dieuze, France). Deionized HPLC-grade water was produced in-house using a Milli-Q water purification system (Millipore, Molsheim, France). 4 x 2 m chip-based pillar array columns (PACs, C_{18}-NH_2) were connected.

C-18 coated porous micro-pillar array columns were acquired from PharmaFluidics (Zwijnaarde, Belgium). The chips contain channels with a length of 2 m and a width of 315 µm. The channels are filled with cylindrical pillars (5 µm diameter, 18 µm deep, 2.5 µm interpillar distance, 59% bed channel porosity, porous layer thickness 450 nm) and were fabricated in the same way as already described in detail by Callewaert *et al*. [27].

2.2 Instrumentation.

Nano-LC experiments were conducted using an UltiMate 3000 RSLC nano system (Thermo Fisher Scientific, Germering, Germany) equipped with a binary high-pressure gradient pump (referred to as NC-pump) with Nano ProFlow flow meter (50-1500 nL/min) located above the pump heads (controls the required partial flows of the two solvent channels so that the selected target flow and the selected solvent composition are reliably met). ProFlow™ technology improves nano flowrate control and results in high retention time precision and higher quality data. UltiMate 3000 RSLC nano system has also ternary low-pressure (LPG) micro pump (referred to as loading pump, it is ideal to be used for on-line sample loading), split-loop autosampler, a forced-air column oven, and a diode-array detector equipped with a 3 nL UV flow cell (10 mm path length). The loading pump was used for sample loading into the 4 nL stainless steel valve. 75 µm ID x 550 mm nano-viper connected to the

fused silica capillary of 50 μm ID x 100 mm via the stainless zero dead volume union was used to connect the NC-pump to a 4-nanoliter injection valve (VICI C4N-4004-.004EUHA). The column outlet tubing was directly connected with a stainless steel zero dead volume union directly to the UV detector. The dwell volume between the autosampler and PACs columns is 24 μL. The total extra-column volume of a nano-LC system (from the 4 nL injection valve to the UV detector cell) is 0.54 μL. All isocratic and gradient phenones separations were performed in triplicate, using a 4 nL injection volume, a column oven temperature of 30 °C, and UV detection at = 260 nm with a data collection rate of 2.5 Hz and a response time of 0.6 s.

2.3 Mobile-phase and sample preparation.

Mobile phase A was Milli-Q water with 0.1% formic acid, mobile phase B was acetonitrile with 0.1% formic acid.

Stock solutions (1000 ppm) of each compound were prepared by dissolving 10.0 mg of each in 50% mobile phase B (50% acetonitrile/water with 0.1% formic acid), which was further completed to 10 mL with the same solvent. Sample mixture for isocratic measurements were prepared by mixing t_0 marker, uracil (5 ppm), butyrophenone (15 ppm) and valerophenone (15 ppm) with 50% mobile phase B. For the gradient separation, a sample containing uracil (30 ppm), acetanilide (130 ppm) and seven phenones: acetophenone (80 ppm), propriophenone (80 ppm), butyrophenone (80 ppm), valerophenone (100 ppm), hexanophenone (140 ppm), heptanophenone (150 ppm), octanophenone (160 ppm) were mixed with 50% mobile phase B.

2.4 Calculations.

The plate count was calculated of half height using European Pharmacopeia: $N=5.54(\frac{t_r}{w_{0.5}})^2$.

Peak capacity based on t_G is calculated based on the length of the gradient: $P_c=1+\frac{t_G}{w}$, where the average peak widths at the baseline of all compounds is taken into account. Peak capacity

based on t_R is calculated based on the actual elution gradient window (running between the first and the ith component of the sample mixture): $P_c=1+\frac{t_i-t_1}{w}$. Only baseline peak width of the last eluting compound (octanophenone) was used for the calculation of t_R-based P_c.

3. Results and discussion.

To determine the optimal flow velocity and the attainable plates, retained and unretained van Deemter plots were obtained (Fig. 1). Minimal plate heights of H=5.0 µm, H=6.3 µm and H=7.7 µm were obtained for uracil (unretained), butyrophenone (k=0.85), and valerophenone (k=1.94) respectively, corresponding to a number of plates N=1.6×10^6, N=1.2×10^6 and N=1.0×10^6. The optimal linear velocities were 0.60 mm/s, corresponding to 150 nl/min for the retained compounds and 0.74 mm/s corresponding to 200 nl/min for the unretained compound and the total run time was about 650 and 510 min in the 4x2 m column, respectively. The observed increase in B-term dispersion at increasing retention could be related to surface diffusion [28]. The decrease of the plate height from uracil (k=0) to butyrophenone (k=0.85) and to valerophenone (k=1.94) is nearly constant irrespective of the linear velocity applied from 0.2 to 1.4 mm/s. Because the C term of such small molecules (D_m ~ 10^{-9} m^2/s) associated to the diffusion across the thin porous shell (450 nm) is small, the difference appears also to be related to the eddy dispersion term.

The (slight) peak tailing is related to coupling dispersion of the outlet capillary and the capillary going to the UV detector. The obtained permeability of the PAC columns was found to be about 3.3 ×10^{-13} m^2, which is much higher than that of packed columns, (ranging from typically 4 ×10^{-15} m^2 to 2.5 ×10^{-14} m^2 for 2 to 5 µm particle columns respectively [29-30], and monolithic columns (typically 9.1×10^{-14} m^2) [31], which leads to much lower pressure drops for the same eluent at the same linear mobile phase velocity. This corresponds to a minimal separation impedance of E=180. In literature, similar plate counts have been obtained by K. Horie *et al.*,

for the tryptic peptides and also for nucleosides sample as a representation of small molecules in a 2 m long silica monolith column, but the separation yielded only a peak capacity (=t_G/t_w, where t_w-peak width (4σ)) of approximately 360 [29]. It appears to be much more challenging to separate small molecules and quite some groups active in (silica) monolith development have focused on this problem yielding promising results, but it remains much easier to obtain high peak capacities with relatively large molecules as peptides. It is indeed well known that for molecules with a high *S*-value much higher peak capacities can be obtained than when working with smaller molecules for a given packing, [32]: Vaast *at al.* reported the maximal peak capacity of 325 in 61 min for complex mixture of small molecules, applying 1200 bar and using coupled columns 60 cm (4×15 cm) packed with 2.6 µm core–shell particles (with Δc= 0.57, t_G/t_0= 15) [33].

To evaluate the peak capacity of our system gradient separations were run at different flow rates near the optimal flow rate (250 nl/min). In Fig. 3, a representative chromatogram is depicted revealing sharp needle-like peaks. In less than 10h, a t_R-based peak capacity of 732 and t_G-based peak capacity of 1103 were obtained. The global influence of gradient time on peak capacity can be seen from Fig. 4, where a t_G-based PC value of approximately n_c= 1815 (t_G= 2050 min) was obtained. When applying a 2050 min gradient a t_R based peak capacity of n_c = 986 was obtained. To assess the theoretical PC limit at longer analysis times the experimental data were fitted with a model from Blumberg [34].

According to Blumberg, the 4σ-based peak capacity can be written as [35]:

$$P_c = 4\sqrt{N}U_{ga}\, ln\frac{U_{ga}^2(r_\Phi^2-6)+6(1+\ r_\Phi\, e^g+U_{ga}X)}{U_{ga}^2\,(r_\Phi^2-6)+6(1+U_{ga}r_\Phi)}$$

$$X = r_\Phi\sqrt{1+(2+r_\Phi)e^g}\ +\frac{e^{2g}}{U_{ga}^2} \quad \text{with} \quad r_\Phi = S\frac{\Delta\Phi}{t_g}t_0, e^g = k_0, U_{ga} = \frac{1}{\sqrt{1+r_\Phi+r_\Phi^2/3}},$$

with N the plate count, U_{ga} the asymptotic utilization of separability, r_ϕ the dimensionless mixing rate [35], g the normalized range of mixing ramp [35], t_g the gradient time and t_0 is the column dead time.

The corresponding time of elution of the last eluting compound of the mixture is given by:

$$t = t_0 \frac{r_\Phi + ln(1 + r_\Phi e^g)}{r_\Phi}$$

In Fig. 4 it can be seen that the experimental peak capacities follow the Blumberg model (experimentally validated in [34]) within a reasonable agreement, indicating our peak capacity measurements on the coupled column system follow the expected behavior.

Inspecting the fitted values at higher gradient times shows that higher PC values can still be achieved. A t_G value of e.g. 3000 min and 5000 min would still produce larger PC values of respectively 2524 and 3209. For such very long separation times the benefit of higher peak capacity needs to be balanced against the gain in peak capacity. The use of longer columns and gradients lengths generally increases peptide identifications and can play a very critical role as a separation method for shotgun proteomics.

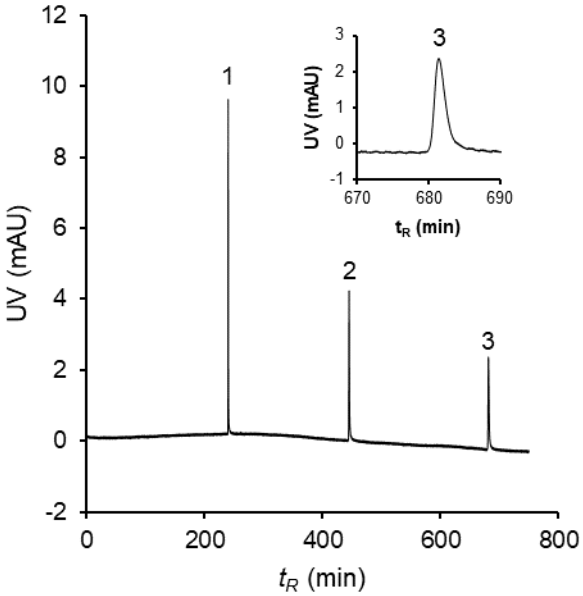

195

196 **Fig.1** Isocratic separation of unretained compound (uracil) and two alkylophenones on an 8 m
197 long column using 30% ACN in water with 0.1% FA at the flow rate of 150 nL/min. Peak
198 identification: (1) uracil, (2) butyrophenone, (3) valerophenone.

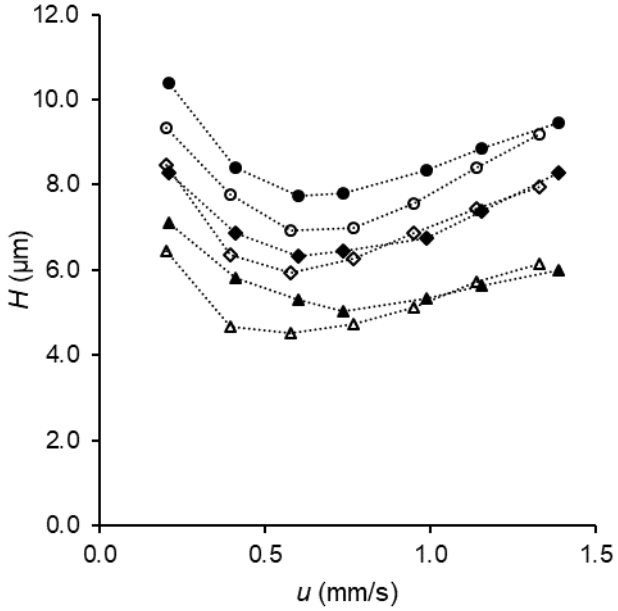

199

200 **Fig. 2** Van Deemter plots of the experimental plate heights of uracil (unretained compound),
201 butyrophenone (retained compound, *k*= 0.85) and valerophenone (retained compound, *k*= 1.94)
202 on 2 m µPAC columns and four connected 2 m long µPAC columns. The triangle corresponds

to uracil, the diamonds corresponds to butyrophenone, and the circles corresponds to valerophenone. Empty shapes represent 2 m µPAC columns, filled shapes represent four connected 2 m long µPAC columns.

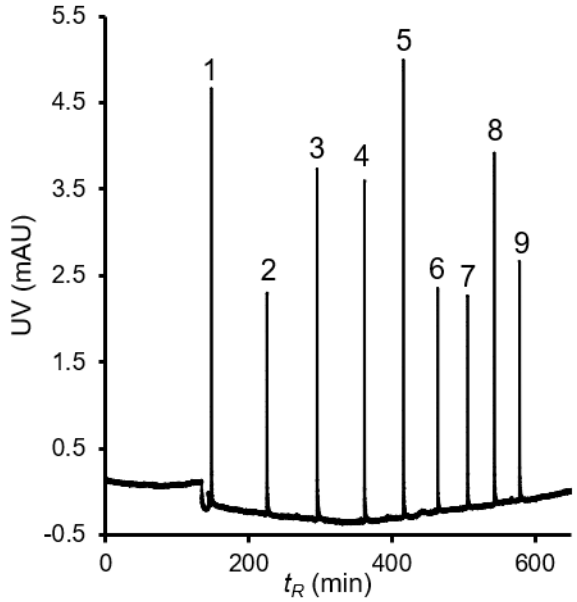

Fig. 3 Chromatogram for 650 min gradient obtained on 4 x 2 m chip-based columns. Sample: uracil (1), acetanilide (2), acetophenone (3), propriophenone (4), butyrophenone (5), valerophenone (6), hexanophenone (7), heptanophenone (8), octanophenone (9); gradient: 2.5-97.5% acetonitrile with 0.1% FA; temperature 30 °C; flow rate 250 nl/min; UV-VIS detection: 260 nm. A peak capacity based on t_R of 732 was achieved.

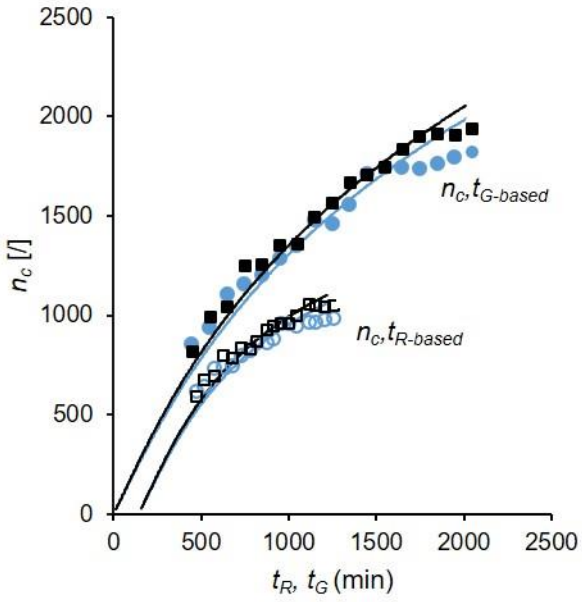

214

215 **Fig. 4** Peak capacities (n_c) for octanophenone and the sample mixture on four connected PAC
216 columns at different gradient time (flow rate of 0.25 µL/min). Black squares correspond to
217 octanophenone, blue circles correspond to sample mixture.

218

219 **REFERENCES**
220

221 [1] Cabooter, D.; Desmet, G. UHPLC in Life Sciences. *RSC Chromatogr. Monographs*, **2012**,
222 16.

223 [2] Blue, L. E., Franklin, E. G., Godinho, J. M., Grinias, J. P., Grinias, K. M., Lunn, D.
224 B.,Moore, S. M. Recent advances in capillary ultrahigh pressure liquid chromatography. *J.*
225 *Chromatogr., A* **2017**, 1523, 17–39.

226 [3] Walter, T. H., Andrews, R. W. Recent innovations in UHPLC columns and instrumentation.
227 *TrAC Trends Anal. Chem.* **2014**, 63, 14–20.

228 [4] Katz, E.; Eksteen, R.; Schoenmakers, P. *Handbook of HPLC*. New York, Basel, **1998**, 78.

[5] Fekete, S.; Schappler, J.; Veuthey, J. L.; Guillarme, D. Current and future trends in UHPLC. *TrAC Trends Anal. Chem.* **2014**, 63, 2–13.

[6] Detobel F.; De Bruyne, S.; Vangelooven, J.; De Malsche, W.; Aerts T.; Terryn, H.; Gardeniers, H.; Eeltink, S.; Desmet, G. Fabrication and chromatographic performance of porous-shell pillar-array columns. *Anal. Chem.* **2010**, 82, 7208-7217.

[7] Eijkel, J. Chip-based HPLC: the quest for the perfect column. *Lab Chip*. **2007**, 7, 815-817.

[8] De Smet, J.; Gzil, P.; Vervoort, N.; Verelst, H.; Baron, G. V.; Desmet, On The Optimisation of the Bed Porosity and the Particle Shape of Ordered Chromatographic Separation Media. G. *J. Chromatogr., A* **2005**, 1073, 43−51.

[9] Knox, J.H.; Saleem, M. Kinetic conditions for optimum speed and resolution in column chromatography. *J. Chromatogr. Sci*. **1969**, 7, 614.

[10] H. Poppe, Some reflections on speed and efficiency of modern chromatographic methods. *J. Chromatogr., A* **1997**, 778, 3-21.

[11] Lincoln D. R.; Charlton J. J.; Hatab N. A.; Skyberg B.; Lavrik N. V.; Kravchenko I. I.; Bradshaw J. A.; Sepaniak M. J. Surface Modification of Silicon Pillar Arrays To Enhance Fluorescence Detection of Uranium and DNA. *ACS Omega* **2017**, 2, 7313−7319.

[12] Gustafsson O.; Mogensen K. B.; Kutter, J. P. Underivatized cyclic olefin copolymer as substrate material and stationary phase for capillary and microchip electrochromatography, *Electrophoresis* **2008**, 29 (15), 3145-3152.

[13] Isokawa, M. Takatsuki, K. Song, YT, Shih, K.; Nakanishi, K.; Xie, ZM.; Yoon, DH.; Sekiguchi, T.; Funatsu, T.; Shoji, S. Liquid Chromatography Chip With Low-Dispersion And Low-Pressure-Drop Turn Structure Utilizing a Distribution-Controlled Pillar Array. *Anal. Chem.*, **2016**, 88 (12), 6485–6491.

[14] Op De Beeck J.; Callewaert M.; Ottevaere H.; Gardeniers H.; Desmet G.; De Malsche W. Suppression of the sidewall effect in pillar array columns with radially elongated pillars. *J. Chromatogr., A* **2014**, 1367, 118-22.

[15] Nissilä T.; Sainiemi L.; Sikanen T.; Kotiaho T.; Franssila S.; Kostiainen R.; Ketola RA. Silicon micropillar array electrospray chip for drug and biomolecule analysis. *Rapid Commun Mass Spectrom*. **2007**, 21 (22), 3677-82.

[16] Guiochon, G. Monolithic columns in high-performance liquid chromatography. *J. Chromatogr., A* **2007**, 1168, 101–168.

[17] De Vos, J.; Stassen, C.; Vaast, A.; Desmet, G.; Eeltink, S. Maximizing the peak capacity using coupled columns packed with 2.6 µm core–shell particles operated at 1200 bar. *J. Chromatogr., A* **2012**, 1264, 57– 62.

[18] Shen, Y.; Smith, R.D.; Unger, K.K.; Kumar, D.; Lubda, D. Ultrahigh-throughput proteomics using fast RPLC separations with ESI-MS/MS. *Anal. Chem*. **2005**, 77, 6692.

[19] MacNair, J.E.; Patel, K.D.; Jorgenson, J.W. Ultrahigh-pressure reversed-phase capillary liquid chromatography: isocratic and gradient elution using columns packed with 1.0-micron particles. *Anal. Chem*. **1999**, 71, 700.

[20] Horie, K.; Sato, Y.; Kimura, T.; Nakamura, T.; Ishihama, Y.; Oda, Y.; Ikegami, T.; Tanaka, N. Estimation and optimization of the peak capacity of one-dimensional gradient high performance liquid chromatography using a long monolithic silica capillary column. *J. Chromatogr., A* **2012**, 1228, 283.

[21] Eugster, P.J.; Biass, D.; Guillarme, D.;Favreau, P.; Stocklin, R.; Wolfender, J.L. Peak capacity optimisation for high resolution peptide profiling in complex mixtures by liquid

chromatography coupled to time-of-flight mass spectrometry: Application to the Conus consors cone snail venom. *J. Chromatogr*., *A* **2012**, 1259, 187.

[22] Rogeberg, M.; Wilson, S.R.; Greibrokk, T.; Lundanes, E. Separation of intact proteins on porous layer open tubular (PLOT) columns. *J. Chromatogr., A* **2010**, 1217, 2782–2786.

[23] Hara, Y.; Izumi, Y.; Nakaoa, M.; Hata, K.; Baron, G.V.; Bamba, T.; Desmet, G. Silica-based hybrid porous layers to enhance the retention and efficiency of open tubular capillary columns with a 5 μm inner diameter. *J. Chromatogr., A* **2018**, 1580, 63-71.

[24] Hara, T.; Futagami, S.; Eeltink, S.; De Malsche, W.; V. Baron, G.; Desmet G. Very High Efficiency Porous Silica Layer Open-Tubular Capillary Columns Produced via in-Column Sol−Gel Processing. *Anal. Chem*. **2016**, 88, 10158−10166.

[25] Sarrut, M.; D'Attoma, A.; Heinisch, H. Optimization of conditions in on-line comprehensive two-dimensional reversed phase liquid chromatography. Experimental comparison with one-dimensional reversed phase liquid chromatography for the separation of peptides. *J. Chromatogr., A* **2015**, 1421, 48–59.

[26] De Malsche, W.; Op De Beeck, J.; De Bruyne, S.; Gardeniers, H.; Desmet, G. Realization of 1 x 10(6) Theoretical Plates in Liquid Chromatography Using Very Long Pillar Array Columns. *Anal. Chem*. **2012**, 84, 1214−1219.

[27] Callewaert, M.; Op De Beeck, J.; Maeno, K.; Sukas, S.; Thienpont, H.; Ottevaere, H.; Gardeniers, H.; Desmet, G.; De Malsche W. Integration of uniform porous shell layers in very long pillar array columns using electrochemical anodization for liquid chromatography. W. *Analyst*, **2014**, 139, 618-625.

[28] Miyabe, K.; Guiochon, G.; Surface diffusion in reversed-phase liquid chromatography. *J. Chromatogr., A* **2010**, 1217, 1713–1734

297 [29] Horie, K.; Kamakura, T.; Ikegami, T.; Wakabayashi, M.; Kato, T.; Tanaka, N.; Y.
298 Ishihama, Y. Hydrophilic interaction chromatography using a meter-scale monolithic silica
299 capillary column for proteomics LC-MS. *Anal. Chem*. **2014**, 86, 3817−3824.

300 [30] Hara, T.; Makino, S.; Watanabe, Y.; Ikegami, T.; Cabrera, K.; Smarsly, B.; Tanaka, N.
301 The performance of hybrid monolithic silica capillary columns prepared by changing feed
302 ratios of tetramethoxysilane and methyltrimethoxysilane. *J. Chromatogr., A*, **2010**, 1217, 89-
303 98.

304 [31] Svec, F. Quest for organic polymer-based monolithic columns affording enhanced
305 efficiency in high performance liquid chromatography separations of small molecules in
306 isocratic mode. *J. Chromatogr., A*, **2012**, 1228, 250-262.

307 [329] Neue, U. D. Peak capacity in unidimensional chromatography. *J. Chromatogr*., *A* **2008**,
308 1184, 107–130.

309 [33] Vaast, A,; De Vos, J.; Broeckhoven, K.;Verstraeten M.; Eeltink, S. Maximizing the peak
310 capacity using coupled columns packed with 2.6 µm core-shell particles operated at 1200 bar.
311 *J. Chromatogr. A* **2012**, 1256, 72– 79.

312 [34] Desmet, G.; Blumberg, L.M. Optimal Mixing Rate in Linear Solvent Strength Gradient
313 Liquid Chromatography. *Anal. Chem*. **2016**, 88, 2281−2288.

314 [35] Desmet, G.; Pepermans V.; Broeckhoven K.; Blumberg L. M. Optimal mixing rate in
315 reverse phase liquid chromatography. Experimental evaluations. *J. Chromatogr. A* **2017**, 1513,
316 84–92.